

Article

The Refined Gravity Field Models for Height System Unification in China

Panpan Zhang^{1,2}, Zhicai Li^{3,4,*}, Lifeng Bao^{1,2}, Peng Zhang⁴, Yongshang Wang⁴, Lin Wu^{1,2} and Yong Wang^{1,2}¹ State Key Laboratory of Geodesy and Earth's Dynamics, Innovation Academy for Precision Measurement Science and Technology, Chinese Academy of Sciences, Wuhan 430077, China; zhangpanpan@asch.whigg.ac.cn; baolifeng@asch.whigg.ac.cn; linwu@apm.ac.cn; ywang@whigg.ac.cn² University of the Chinese Academy of Sciences, Beijing 100049, China.³ China University of Mining and Technology-Beijing, Beijing 100083, China. Email: zcli@cumtb.edu.cn⁴ National Geomatics Center of China, Beijing 100830, China; zhangpeng@ngcc.cn; ys@ngcc.cn

* Correspondence: zcli@cumtb.edu.cn; Tel.: +86-0278-6752107

Abstract: A unified height datum is essential for global geographic information resource construction, ecological environment protection and scientific research. The goal of this paper is to derive the geopotential value for the Chinese height datum (CNHD) in order to realize the height datum unification in China. The estimation of height datum geopotential value usually depends on high-precision global gravity field models (GFM). The satellite gravity missions of the Gravity Recovery and Climate Experiment (GRACE) and Gravity field and steady-state Ocean Circulation Exploration (GOCE) provide high-accuracy medium-long wavelength gravity field spectrum, but satellite-only GFM are limited to medium-long wavelengths which will involve the omission errors. To compensate for the omission errors in satellite-only GFM, a spectral expansion approach is used to obtain the refined gravity field models using the EGM2008 (Earth Gravitational Model 2008) and residual terrain model (RTM) technique. The refined GFM are evaluated by using high-quality GNSS/levelling data, the results show that the quasi-geoid accuracy of the refined DIR_R6_EGM2008 RTM model in China has the optimal accuracy, and compared with the EGM2008 model and the DIR_R6 model, this refined model in China is improved by 9.6 cm and 21.8 cm, and the improvement ranges are 35.7% and 55.8%, respectively. Finally, the geopotential value of the Chinese height datum is estimated to be equal to $62636853.29 \text{ m}^2\text{s}^{-2}$ with respect to the global reference level defined by $W_0=62636853.4 \text{ m}^2\text{s}^{-2}$ by utilizing the refined DIR_R6_EGM2008_RTModel and 1908 high-quality GNSS/levelling datapoints.

Citation: Lastname, F.; Lastname, F.; Lastname, F. Title. *Remote Sens.* **2022**, *14*, x. <https://doi.org/10.3390/xxxxx>

Academic Editor: Firstname Lastname

Received: date

Accepted: date

Published: date

Publisher's Note: MDPI stays neutral with regard to jurisdictional claims in published maps and institutional affiliations.



Copyright: © 2022 by the authors. Submitted for possible open access publication under the terms and conditions of the Creative Commons Attribution (CC BY) license (<https://creativecommons.org/licenses/by/4.0/>).

1. Introduction

With the emergence of Global Navigation Satellite System (GNSS), users can obtain consistent ellipsoidal height at global scale. The ellipsoid height relative to a given geocentric ellipsoid can be obtained quickly and accurately by using GNSS. However, the ellipsoidal height is not related to the Earth's gravity field. The height related to the Earth's gravity field usually refers to the orthometric or normal height, which is strictly based on the geopotential number C_P ($C_P = W_0^{LVD} - W_P$, where W_0^{LVD} is the geopotential value for the local vertical datum, and W_P indicates the gravity potential for point P). The local vertical datum refers to the geoid (or quasi-geoid), which is assumed to be coincident with the local mean sea level (MSL). Importantly, even though all local height datums are related to the MSL, the vertical offsets between them may be up to 2 m at global scale [1]. This is due to the fact that the MSL presents geographical and time-dependent variations,

but they are a consequence of the natural sea dynamics. Therefore, the vertical datums vary among countries or regions, affecting and restricting the sharing and exchange of global geo-spatial information, the unification of the height datums has become a key point in the field of geodesy.

According to the Global Geodetic Observing System (GGOS) of the International Association of Geodesy (IAG), a global vertical datum related to Earth's gravity field should be established. One of the main works of GGOS is to support global geometric and physical heights with centimeter accuracy within a global framework, and to unify all existing physical height systems [2,3]. A global reference system defines constants, conventions, models, and parameters as the necessary basis for the mathematical representation of geometric and physical quantities [4]. According to the IAG resolution No 1, 2015, the gravity potential value for the International Height Reference System (IHRS) is released equal to $62636853.4 \text{ m}^2\text{s}^{-2}$ [5–7]. According to this resolution, the existing local vertical datum systems can be integrated into the IHRS, which will ensure the consistency of the global height datum systems. The fundamental approach for height datum unification is the Geodetic Boundary Value Problem (GBVP) method [8–13]. This method has been widely applied in areas with good coverage of surface gravity data. However, in areas where surface gravity data are poor or restricted, a feasible option for height datum unification is to use of high-accuracy GFM. The GFM provide expected accuracy at scales from centimeter to decimeter [11]. With the development of high-precision and high-resolution global gravity field models, the GFM has become feasible for the unification of vertical datums [14–22].

The GFM has many advantages for determining the geopotential values of vertical datums, but the results depend largely on the accuracy of the utilized GFM. The satellite gravity missions such as GRACE [23] and GOCE [24] provide unprecedented information for the medium wavelength gravity field [25–26], which can improve the accuracy of medium and long wavelength geoid. The primary goal of the GOCE satellite is to derive about 1–2 cm geoid accuracy to a target resolution of about 100 km [27]. The GRACE/GOCE-based GFM have the medium-long wavelength information with high precision; however, these models have certain omission errors. The omission error for geoid (quasi-geoid) height reaches about 32 cm for a GFM up to degree 200 according to Kaula's rule and the variance model of Tscherning & Rapp [28–31]. This omission error cannot be ignored for realizing the height datum unification. In addition to the omission errors of the GFM, the spectral accuracy of the selected GFM, the uncertainties of GNSS-derived ellipsoidal heights, and the accumulation levelling errors must be considered to determine the vertical datum geopotential with a high accuracy.

The Chinese vertical datum is determined by the MSL observed by the Qingdao tide gauge station during the 27 years from 1952 to 1979. The latest first-order levelling network in China, which is based on the 1985 vertical datum and was completed and put into use in 2017, is the most accurate and practical national modern vertical control network to date [32]. It is used for transmitting normal height at national scale. The aim of the paper is to determine the vertical datum geopotential of China based on the GFM by utilizing the latest normal height results. Thus, the 1985 vertical datum in China can be connected to the IHRS, which can provide a unified height datum for the construction of global geographic information resources, ecological environmental protection and scientific research. In order to derive more accurate height datum geopotential of China based on GFM, we utilize the spectral expansion method by augmenting the GOCE/GRACE-based GFM with the EGM2008 model and residual terrain model (RTM) technique [33–37], which can reduce the omission error of the satellite-only GFM. In addition, considering the large east-west span in China, the systematic accumulated error may occur in the long-distance levelling, and GFM have certain systematic errors between the east and west of China, which has influence on determining the geopotential value of the Chinese height datum. This paper will further analyze the systematic errors influence. Finally, we will

combine the refined GFM^s and GNSS/levelling to preliminarily derive the geopotential value of the Chinese height datum (CNHD) towards height system unification in China. 98
99

The structure of the manuscript is as follows. The materials and method for estimating the Chinese height datum geopotential value is introduced in Section 2. Section 3 provides the results of the Chinese height datum geopotential value and specifically focused on (a) spectral accuracy of GFM^s, (b) the omission errors of the satellite-only GFM^s in China, and (c) the determination of the refined GFM^s. Finally, discussion and conclusions are provided in Section 4 and Section 5, respectively. 100
101
102
103
104
105

2. Materials and Methods 106

2.1. Materials 107

This section briefly introduces the materials used in this study. The main data required are: 1) GNSS/levelling data; 2) global gravity field models; and 3) topographic data. 108
109

2.1.1. GNSS/levelling data 110

The leveling networks in China contain the first, second, third and fourth orders leveling networks. The latest first-order leveling network observations, which was completed and put into use in 2017, are used. This first-order leveling network consists of 148 loops with a length of over 125746.5 km. Considering the large east-west span in China, the systematic accumulated error may occur in the long-distance levelling, therefore, the leveling data is handled by the least square adjustment in which the length correction of levelling rod, the non-parallel correction of level surface, the gravity reduction are considered [32]. The maximum error in leveling is only about 3.57 cm (about 6185 km from Qing-dao leveling origin) after adjustment. Finally, 1908 high-accuracy and evenly distributed GNSS/levelling datapoints are made available by the National Geomatics Center of China to determine the vertical datum geopotential of China. The GNSS ellipsoidal coordinates are based on ITRF2014 [38], and the GNSS coordinate accuracy reaches the millimeter level, in particular, the accuracy of GNSS ellipsoidal heights is about 5 mm. The distribution for the GNSS/levelling datapoints in China is shown in Figure 1. 111
112
113
114
115
116
117
118
119
120
121
122
123
124

Because the GNSS ellipsoidal height is based on a tide-free system, to ensure that the GNSS/levelling-based quasi-geoid height represents a tide-free system, the normal heights are transformed to the tide-free system by following equation [39]: 125
126
127

$$H^{TF} = H^{MF} + 0.68(0.099 - 0.296 \sin^2 \varphi) \quad (1) \quad 128$$

where H^{TF} represents the tide-free normal height, H^{MF} is the mean tide normal height, and φ is the latitude of the GNSS/levelling points. 129
130

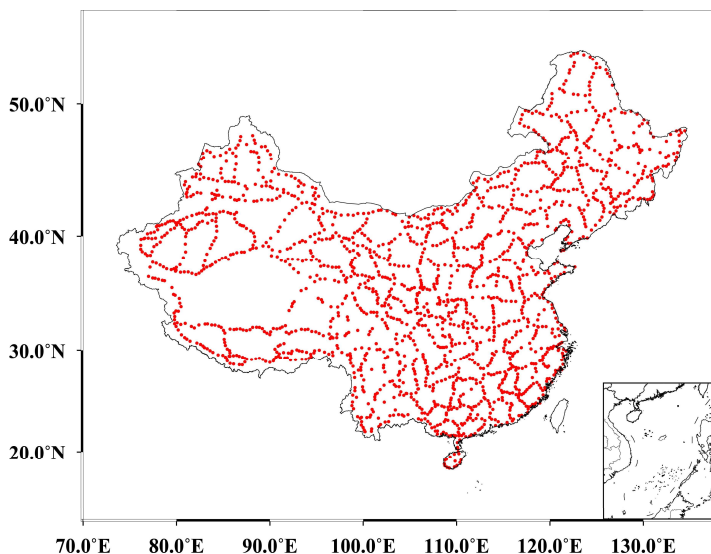


Figure 1. Distribution of GNSS/levelling benchmarks

131

132

2.1.2. Global gravity field Models (GFM)

133

Table 1 shows the GFM used in this paper. The direct approach is employed to derive the DIR_R5 and DIR_R6 models using GOCE satellite gravity observations, GRACE satellite gravity observations and satellite laser ranging (SLR). The DIR_R5 model utilizes GOCE data from Nov 2009-Oct 2013 and GRACE data from the ten years period (2003–2012). The DIR_R6 model utilizes GOCE data from Oct 2009-Oct 2013 and GRACE data from Jan 2007-Nov 2014. The TIM_R5 and TIM_R6 models are derived by the time-wise approach using GOCE observations from Nov 2009-Oct 2013 and Sept 2009-Oct 2013, respectively. The EGM2008 model combines multi-source gravity observation data to derive a maximum degree of 2190, however, this model is complete to d/o 2159. The gravity data utilized in EGM2008 model mainly refers to global gravity database of 5'×5'. The surface gravity data covering China is composed of two-divisions: one is the gravity data of 5' for construction of the EGM2008, without any restrictions, the main coverage areas include Eastern, Southern and Central China; another gravity data resource is permitted to use at a resolution of 15 arc-minute, these data cover other regions except for Eastern, Southern and Central China.

134

135

136

137

138

139

140

141

142

143

144

145

146

147

148

For the consistency of tide system, the \bar{C}_{20} coefficient of GFM is transformed to tide-free system using the following formula [40]:

149

150

$$\bar{C}_{20}^{TF} = \bar{C}_{20}^{ZT} - k_{20} \cdot \langle \Delta \bar{C}_{20} \rangle \quad (2) \quad 151$$

where \bar{C}_{20}^{TF} and \bar{C}_{20}^{ZT} are the spherical harmonic coefficient under the tide-free system and the zero-tide system, respectively, $k_{20} = 0.30190$ is loading Love number, and $\langle \Delta \bar{C}_{20} \rangle = -1.391412 \cdot 10^{-8}$ represents the value of tidal correction.

152

153

154

155

156

157

158

159

160

161

Table 1. The details for global gravity field models. The letter ‘S’ in third column represents satellite data, ‘G’ represents ground observations, ‘A’ represents altimetry observations, and ‘d/o’ represents degree/order.

Models	d/o	Data	Tide system	Reference
EGM2008	2160	S(Grace), G, A	Tide-free	[41]
GO_CONS_GCF_2_TIM_R5	280	S(Goce)	Tide-free	[42]
GO_CONS_GCF_2_TIM_R6	300	S(Goce)	Zero-Tide	[43]
GO_CONS_GCF_2_DIR_R5	300	S(Goce, Grace, Lageos)	Tide-free	[44]
GO_CONS_GCF_2_DIR_R6	300	S(Goce, Grace, Lageos)	Tide-free	[45]

2.1.3. Topographic data

Topographic data are used to calculate the RTM effect and recover the high-frequency gravity signals of missing in the GFM. The RTM represents the difference between the topographic surface and the long-wavelength reference terrain. The Shuttle Radar Topographic Mission (SRTM) V4.1 data [46] with a spatial resolution of $7.5'' \times 7.5''$ are used to represent the land over China. For the sea area, the SRTM15_PLUS V2 topographic data [47] are used, with a spatial resolution of $15'' \times 15''$. The rock-equivalent topography model RET2012 [48] works as the reference topography, the reference terrain elevations can be computed by Equation (2) in [49]. In the coastal zone, the mass-density of seawater is different from that of the standard topographic mass density. To avoid the necessity of distinguishing density changes in the computational process, the rock-equivalent topography (RET) method can be used to compress the water depth to the equivalent rock height [50].

$$H^* = H(1 - \rho_w / \rho) \quad (3)$$

where H^* and H are the compressed water depth and the original water depth, respectively, ρ_w denotes the density of seawater, and ρ represents the standard topographic mass density.

The SRTM and SRTM15_PLUS data can be merged to obtain the unified topographic data on land and sea. The merging process is mainly divided into two steps: (1) the bicubic interpolation method is employed to interpolate the sea topographic data into a spatial resolution of $7.5'' \times 7.5''$, and Equation (3) is employed to process the sea water depths; (2) the land topographic data are combined with the water depth data obtained by step (1). Figure 2(a) shows the merged topography. The residual topographic masses (RTM elevations) are the difference between the SRTM merged data (Figure 2a) and the reference terrain. Figure 2(b) shows the residual terrain model elevations.

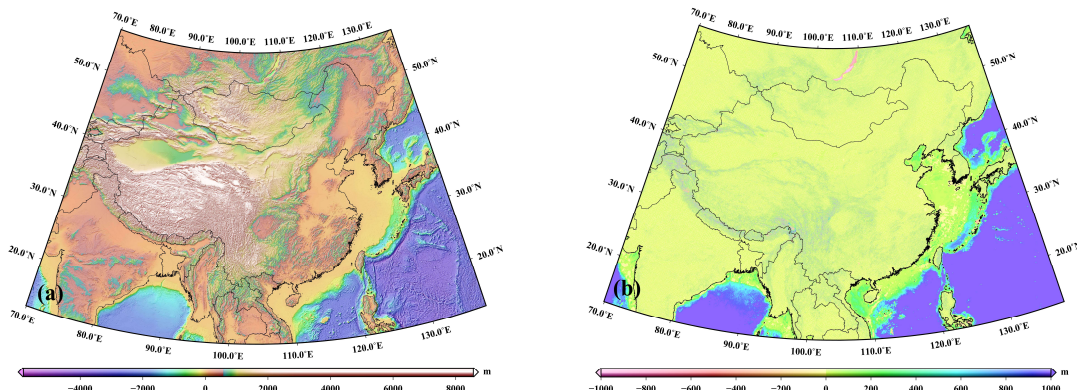


Figure 2. (a) Topography based on merged SRTM and (b) residual terrain model (RTM) elevations with RET2012 terrain as the reference surface.

2.2. Methods for determining the height datum geopotential value

193

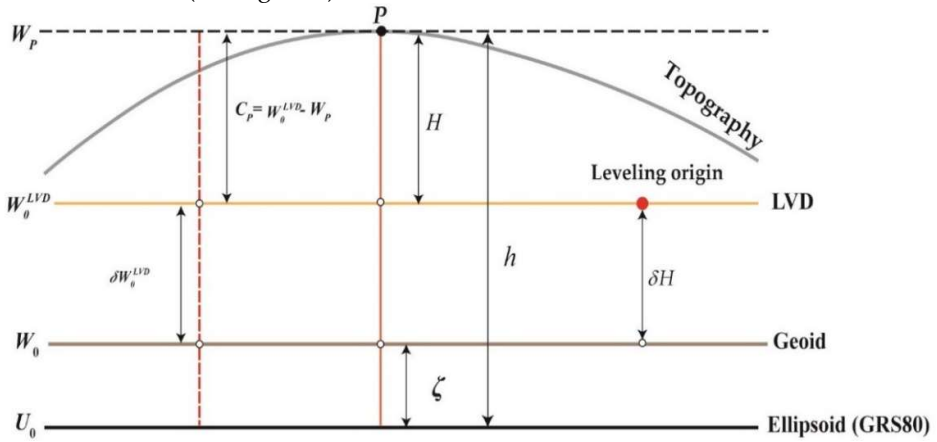
The vertical offset δH between the local height datum and the global geoid can be expressed as:

$$\delta H = h - H - \zeta \quad (4) \quad 196$$

where H represents the normal heights, h is the ellipsoidal heights, and ζ is the height anomalies from GFM (see Figure 3).

197

198



199

Figure 3. The relations among different reference datum surfaces.

200

The height anomaly ζ can be calculated by using the satellite-only GFMs, but the resulting omission errors cannot be ignored. Therefore, the EGM2008 model can be used to extend the satellite-only GFMs to obtain the refined GFMs via the spectral expansion approach. The height anomaly ζ_{GGM} determined by the refined GFMs can be expressed as:

201

202

203

204

205

$$\zeta_{GGM} = \left(\frac{GM - GM_0}{r \cdot \bar{\gamma}} - \frac{W_0 - U_0}{\bar{\gamma}} \right) + \zeta_{GOCE/GRACE} \Big|_2^l + \zeta_{EGM2008} \Big|_{l+1}^{2160} \quad (5) \quad 206$$

where $\zeta_{GOCE/GRACE} \Big|_2^l$ is the height anomaly determined by the satellite-only GFMs truncated to the degree l , and $\zeta_{EGM2008} \Big|_{l+1}^{2160}$ is the height anomaly represented from degrees 201 to 2160 of EGM2008. $GM_0 = 3.986005000 \times 10^{14} \text{ m}^3 \text{s}^{-2}$ and $U_0 = 62636860.8500 \text{ m}^2 \text{s}^{-2}$ are constants of the gravitational constant and the normal potential value of the GRS80 ellipsoid [51], respectively; r is the geocentric radial for computation point; GM represents geocentric gravitational constant used in the GFM; $\bar{\gamma}$ is the mean normal gravity; and $W_0 = 62636853.4 \text{ m}^2 \text{s}^{-2}$ is the geopotential value of the global geoid [52].

207

208

209

210

211

212

213

The RTM technology is used to recover the short-scale signal beyond degree 2160 in Equation (5). The RTM represents the difference (residual terrains) between the topographic surface and the reference surface. The gravitational potentials of residual terrains can be expressed as follows [53]:

214

215

216

217

$$T = G\rho \int_{\Omega} \frac{1}{r} d\Omega \quad (6) \quad 218$$

where T is the gravitational effect for the residual terrains, G denotes the gravitational constant, r is the distance between the attraction mass and the computation point, Ω is the volume for the residual terrains, and ρ is the standard topographic mass density.

219

220

221

The residual terrains are decomposed into a set of rectangular-prism mass. Figure 4 show the coordinate system definition of a rectangular-prism mass body. The computation point P as the origin of this coordinate system, this means that the coordinates

222

223

224

defining have to be transformed by a shift (see Eq. 1 in [54]). To obtain the gravitational effects of a residual mass distribution, The result of Equation (6) for a single rectangular-prism can be calculated using the following equation:

$$T(P) = G\rho \int_{x_1}^{x_2} \int_{y_1}^{y_2} \int_{z_1}^{z_2} \frac{1}{r} dx dy dz = G\rho \left[xy \ln(z+r) + yz \ln(x+r) + zx \ln(y+r) - \frac{x^2}{2} \tan^{-1}\left(\frac{yz}{xr}\right) - \frac{y^2}{2} \tan^{-1}\left(\frac{xz}{yr}\right) - \frac{z^2}{2} \tan^{-1}\left(\frac{xy}{zr}\right) \right]_{x_1}^{x_2} |_{y_1}^{y_2} |_{z_1}^{z_2} \quad (7)$$

where x_1, x_2, y_1, y_2, z_1 , and z_2 describe the corner coordinates of the prism faces in Figure 4.

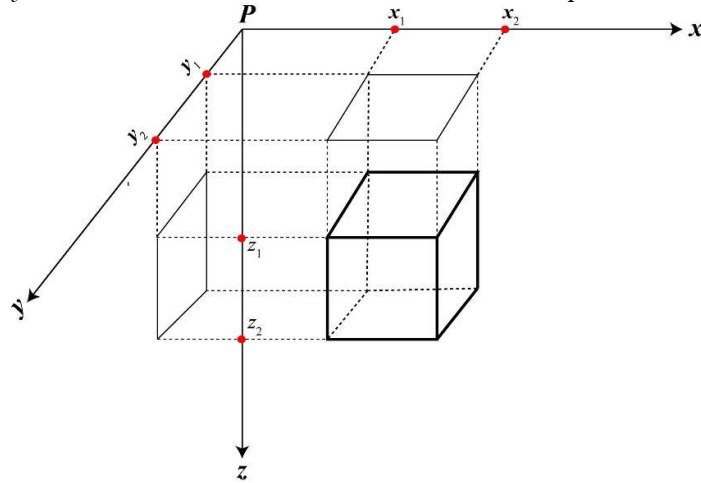


Figure 4. Definition of a prism mass body.

The total gravitational effects of the residual terrains for computation point are derived by a summation of gravitational effects in Equation (7):

$$T(P) = \sum_{i=1}^M T(P)_i \quad (8)$$

where M represents the number for prism mass elements.

The height anomaly ζ_{RTM} caused by the residual mass distribution can be expressed by

$$\zeta_{RTM} = \frac{T(P)}{\gamma_p} \quad (9)$$

where γ_p is normal gravity for computation point P .

ζ_{RTM} represents the quasi-geoid height signals of the GFM beyond degree 2160. Then, the height anomaly ζ determined by the refined GFMs can be further expressed as follows:

$$\zeta = \zeta_{GGM} + \zeta_{RTM} = \left(\frac{GM - GM_0}{r\bar{\gamma}} - \frac{W_0 - U_0}{\bar{\gamma}} \right) + \zeta_{GOCE/GRACE} |_2^l + \zeta_{EGM2008} |_{l+1}^{2160} + \zeta_{RTM} \quad (10)$$

The global or local vertical datum is a gravitational equipotential surface. Therefore, the vertical datum offset determined by Equation (4) should theoretically be a fixed constant. However, vertical offsets contain certain discrepancies due to the influences of systematic errors and random errors. Systematic errors may contain possible systematic errors in GFM, accumulated levelling errors and the GNSS height ellipsoidal errors [55–57]. To reduce these random and systematic errors, the vertical datum offset is estimated by applying a planar correction parametric model. For each GNSS/levelling point P , the observation equation can be formulated as follows:

$$l_p = h_p - H_p - \zeta_p = \delta \bar{H} + a_1 (B_p - B_0) + a_2 (L_p - L_0) \cos B_p \quad (11)$$

where $\delta\bar{H}$ is the unknown height datum offset, (B_p, L_p) are the geodetic coordinates for the computation point, (B_0, L_0) are the geodetic coordinates for leveling origin in the local vertical datum zone, and a_1 and a_2 are the north-south tilt and east-west tilt, respectively. If there are n GNSS/levelling benchmarks in the local vertical datum zone, according to Equation (11), the function model can be expressed as follows:

$$\underbrace{\begin{bmatrix} h_1 - H_1 - \zeta_1 \\ h_2 - H_2 - \zeta_2 \\ \vdots \\ h_n - H_n - \zeta_n \end{bmatrix}}_A = \underbrace{\begin{bmatrix} 1 & (B_1 - B_0) & (L_1 - L_0) \cos B_1 \\ 1 & (B_2 - B_0) & (L_2 - L_0) \cos B_2 \\ \vdots & \vdots & \vdots \\ 1 & (B_n - B_0) & (L_n - L_0) \cos B_n \end{bmatrix}}_A \cdot \underbrace{\begin{bmatrix} \delta\bar{H} \\ a_1 \\ a_2 \\ x \end{bmatrix}}_x \quad (12) \quad 258$$

The unknown parameter x in Equation (12) can be further determined according to the least square adjustment of the system denoted by

$$x = (\mathbf{A}^T \mathbf{P} \mathbf{A})^{-1} \mathbf{A}^T \mathbf{P} \mathbf{l} \quad (13) \quad 261$$

where $\mathbf{P} = \mathbf{D}_{ll}^{-1}$ is the weight matrix, \mathbf{D}_{ll} represents the error variance-covariance matrix for the observed values. Assuming the involved terms in Equation (11) is uncorrelated each other, the \mathbf{D}_{ll} can be specified by

$$\mathbf{D}_{ll} = \mathbf{D}_{hh} + \mathbf{D}_{HH} + \mathbf{D}_{\zeta\zeta} \quad (14) \quad 265$$

where \mathbf{D}_{hh} and \mathbf{D}_{HH} are the error variance-covariance matrix of the ellipsoidal and normal heights, respectively, and $\mathbf{D}_{\zeta\zeta}$ represents the error variance-covariance matrix for quasi-geoid heights.

$\mathbf{D}_{\zeta\zeta}$ might be determined from the errors of the GFMs and RTM quasi-geoid heights. Voigt and Denker [58] and Grombein et al. [17] showed that the uncertainty of the topography-implied gravity signals is at the sub-mm level, therefore, the errors of RTM quasi-geoid heights can be considered negligible. However, the error variance-covariance matrix of the GFM might generally not be available [17]. In addition, the uncertainties for ellipsoidal heights and normal heights are usually not available. Therefore, it is not possible to obtain \mathbf{D}_{ll} in practical cases. Based on the above reasons, we assume $\mathbf{P}=\mathbf{I}$ in this paper, where \mathbf{I} is the identity weight matrix.

After removing the errors effects, we will get vertical offsets with considering corrections by:

$$\delta H_p = (h_p - H_p - \zeta_p) - a_1 (B_p - B_0) - a_2 (L_p - L_0) \cos B_p \quad (15) \quad 279$$

The geopotential value W_{p0}^{LVD} for point P can be expressed as follows:

$$W_{p0}^{LVD} = W_0 - \delta H_p \cdot \bar{\gamma}_p \quad (16) \quad 281$$

where $\bar{\gamma}_p$ denotes the mean normal gravity, which is computed by Equation (4-60) in [59].

Finally, we can derive the geopotential value W_0^{LVD} of the local height datum by:

$$W_0^{LVD} = W_0 - \frac{\sum_{p=1}^m \delta H_p \cdot \bar{\gamma}_p}{m} = W_0 - \delta W_0^{LVD} \quad (17) \quad 285$$

where m is the number of GNSS/levelling benchmarks.

3. Results

3.1. Spectral accuracy evaluation for GFMs

According to the spherical harmonic coefficients and their formal errors, the spectral accuracy of a GFM is evaluated by using the commission errors (the degree error, cumulative degree error, difference degree error and cumulative difference degree error) and signal-to-noise ratio (SNR). The geoid degree error can be expressed as the square root of the error degree variances, the cumulative geoid degree error is represented as the square root of the cumulative geoid error degree variances. A relative comparison of satellite-based GFM and EGM2008, can be estimated by the difference degree error and the cumulative difference degree error. These specific calculation formulas can be found in [60].

Figure 5(a) shows the geoid degree errors for GFMs. We can find from the figure that the geoid degree errors of the satellite-only GFMs before about degree 200 are lower than the degree error of EGM2008. Figure 5(b) shows the geoid cumulative degree errors for the GFMs. The geoid cumulative degree errors for DIR_R5 and DIR_R6 models are lower than that of the EGM2008 model in the whole spectral domain. The geoid cumulative degree errors for TIM_R5 and TIM_R6 models are lower than that of the EGM2008 model before approximately degree 260. The above analysis shows that the satellite-only GFMs have higher medium-long wavelength accuracy than the EGM2008 model and the satellite-based GFMs are characterized by noise as increases in degree.

Figure 6(a) indicates the SNRs for the GFMs. The SNRs of satellite-only GFMs are better than that of the EGM2008 model before about degree 200. The results show that the satellite-only GFMs have a strong geoid signal in the medium-long wavelength band, and the EGM2008 model has a strong geoid signal in the short wavelength band. Figure 6(b) shows the difference degree error and cumulative difference degree error of the satellite-only GFMs taking the EGM2008 model as a reference. We can find from the figure that the geoid difference degree errors for DIR_R5 and DIR_R6 are lower than geoid difference degree errors of the TIM_R5 and TIM_R6 before about degree 100 and cumulative geoid difference degree errors of the DIR_R5 and DIR_R6 are lower than cumulative difference degree errors of TIM_R5 and TIM_R6 before about degree 150. This is because the DIR_R5 and DIR_R6 GFM take advantage of GRACE gravity data and LAGEOS satellite laser ranging (SLR) data.

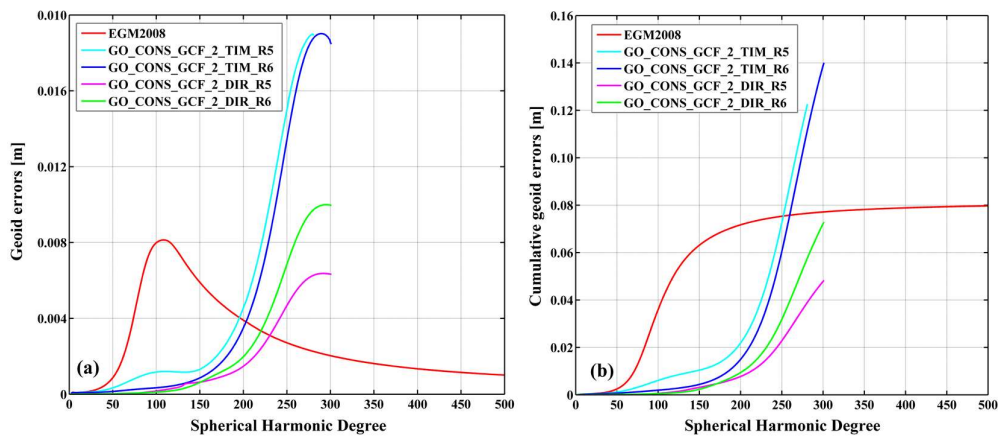


Figure 5. (a) Geoid degree error and (b) cumulative geoid degree errors for GFMs

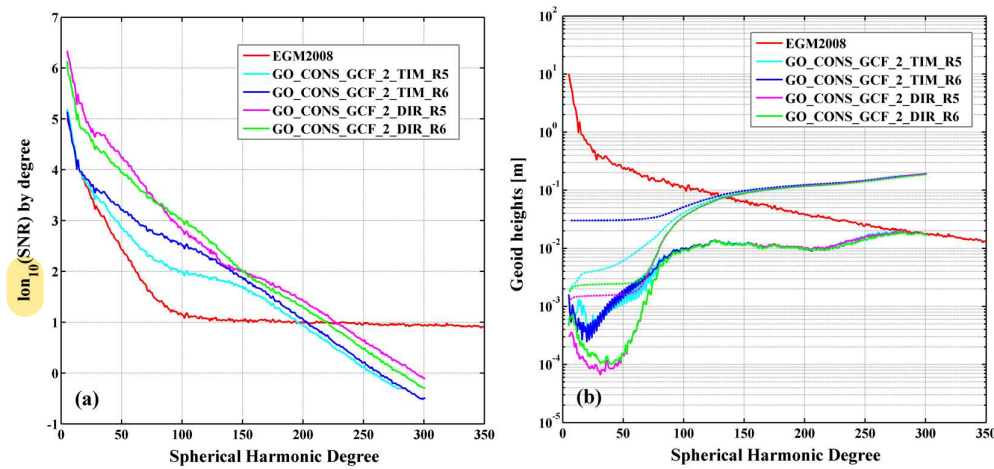
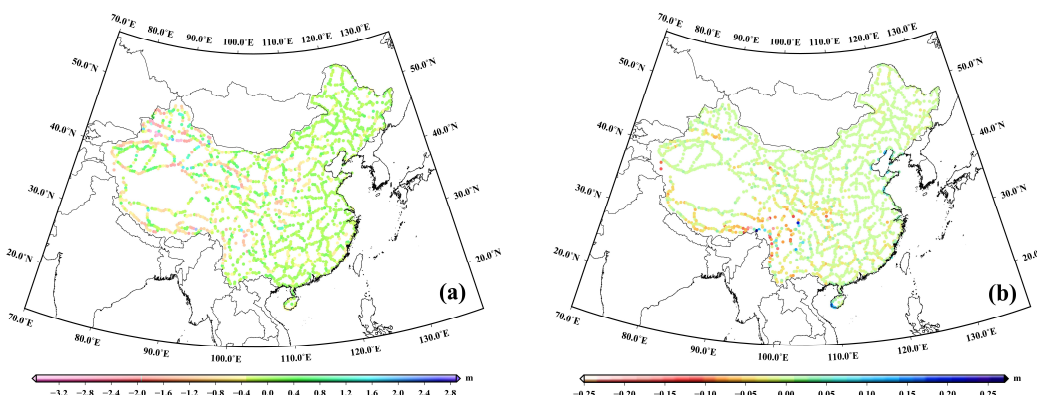


Figure 6. (a) Signal to noise ratios (SNRs) of GFMs and (b) difference degree errors (solid-line) and difference cumulative degree errors (dashed-line) between satellite-only GFMs and the EGM2008.

3.2. The omission errors for satellite-only GFMs

The satellite-only GFMs have high spectral accuracy and strong geoid signals. However, the maximum expansion degree of these satellite-based models is limited and there are certain omission errors as a result of the gravity field attenuation at the height of satellite orbit. To quantify the magnitudes of these omission errors of satellite-only GFMs, we assume that 200 is the general expansion degree of the satellite-only GFM. The magnitudes of the height anomaly $\zeta_{201-2160}^{\text{EGM2008}}$ using the degrees 201 to 2160 of EGM2008 and the height anomaly ζ_{RTM} inferred from the RTM can indicate the omission errors of the satellite-only GFM. The specific calculation process for ζ_{RTM} can be found in section 4.3.

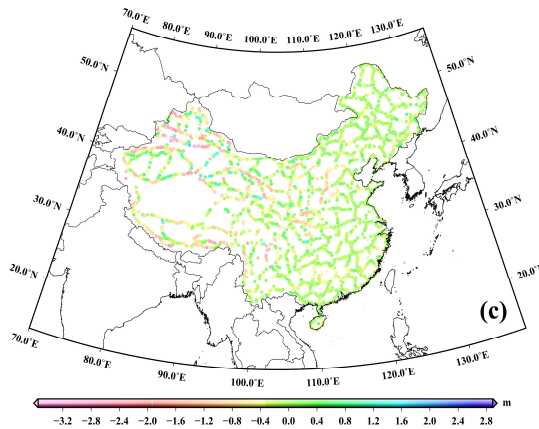
Figure 7(a) indicates the omission error of satellite-only GFM represented by $\zeta_{201-2160}^{\text{EGM2008}}$, Figure 7(b) shows the omission errors of satellite-only GFM represented by ζ_{RTM} , and Figure 7(c) shows the total omission errors obtained from the sum of $\zeta_{201-2160}^{\text{EGM2008}}$ and ζ_{RTM} . Table 2 show statistics for the omission errors of satellite-only GFM in China. We can find from the figure that the omission errors in the rugged regions are larger (mid-west of mainland China) than in other regions. From Table 2, we can find that the omission errors of the satellite-only GFM in mainland China reach the decimeter level, and the largest amplitude is about 350 cm. The omission error signals represented by the RTM is centimeter level in mainland China. Therefore, the omission errors for the satellite-only GFMs must be considered for unification of China vertical datum.



320
321
322

323
324
325
326
327
328
329
330
331
332
333
334
335
336
337
338
339
340
341

342



343

Figure 7. (a) Omission errors of satellite-only GFMs represented by $\zeta_{201-2160}^{EGM2008}$ (b) Omission errors for satellite-only GFMs represented by ζ_{RTM} , (c) Total omission errors of satellite-only GFMs. 344
345

Table 2. Statistics of the omission errors for satellite-only GFMs in China. Unit: (m). 346

Omission errors (m)	Max	Min	Mean	Std
$\zeta_{201-2160}^{EGM2008}$	2.885	-3.529	-0.215	0.601
ζ_{RTM}	0.264	-0.248	-0.006	0.027
$\zeta_{201-2160}^{EGM2008} + \zeta_{RTM}$	2.892	-3.548	-0.221	0.602

3.3. The refined GFMs obtained by the spectral expansion approach

The above spectral validation results show that the satellite-only GFMs have higher spectral accuracy and stronger geoid signals at medium-long wavelength, and EGM2008 model has stronger geoid signals in short wavelength. Therefore, combining the GRACE/GOCE-based GFMs and EGM2008 model to obtain refined GFMs is a feasible strategy.

Because the degree errors of the satellite-only GFMs increase with the increase in degree and order, the noise starts to dominate the signals at high degree and order. Therefore, it is not possible to derive an optimal GFM by combining the maximum degree of satellite-based GFMs and EGM2008. It is not reasonable strategy to get a refined GFM by combining two models directly, and the choice of the optimal degree for the combination is very important. The specific steps used to determine the optimal combination degrees are as follows: (a) the satellite-only GFMs are truncated to degree l ($l=10, 20, 30, \dots, N$, where N is the maximum degree for satellite-only GFMs) as the $0-l$ degree of the refined GFMs, and the $l \sim 2160$ degree of the refined GFMs is supplemented by the corresponding degree of the EGM2008 model; (b) the GNSS/levelling-based height anomaly is used to check the height anomaly determined by the refined GFMs; (c) the combination degree presenting the best accuracy is chosen as the optimal combination degree of the refined GFMs. Figure 8 indicates the standard deviations of the height anomalies differences between GNSS/levelling and the refined GFMs with varying combinations of degree. As seen from Figure 8, the accuracy of the combined GFMs is basically consistent with that of the EGM2008 model before about degree 90. From degree 90 onwards, there are obvious differences in accuracy. We select the optimal combination degree when the standard deviations minimized. Figure 8 shows that 230, 240, 220 and 240 are the optimal combination degree for obtaining the refined GFMs by combining the TIM_R5, TIM_R6, DIR_R5, and DIR_R6 models, respectively, with the EGM2008 model. The accuracy trend in Figure 8 mainly depends on EGM008 model the satellite-only GFMs and GNSS/levelling resources. The GNSS/levelling have a good accuracy and quality, especially, the systematic errors in

347

348

349

350

351

352

353

354

355

356

357

358

359

360

361

362

363

364

365

366

367

368

369

370

371

372

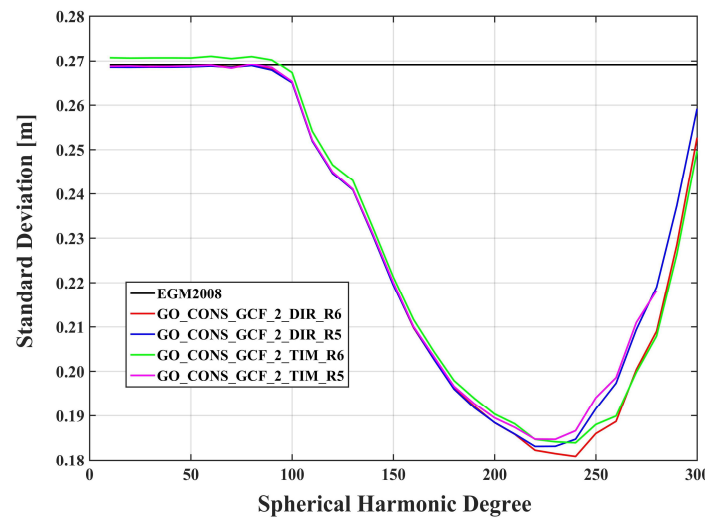
373

374

levelling have been greatly weakened by height network adjustment. Therefore, the results presented in Figure 8 mainly reflects the accuracy of the combined GFM_s in China. The accuracy of the combined GFM_s relies heavily on the improvement of the satellite-only models. Gruber and Willberg [61] demonstrated that 80% accuracy improvement for high-resolution GFM_s compared with EGM2008 reveal the contribution of GOCE solution to medium wavelengths. Therefore, high-quality GNSS/levelling resources and the satellite-only GFM_s increase the quality and reliability of the combined GFM_s in this study.

The RTM technology can further be utilized to obtain higher frequency gravity field signals of the refined GFM_s. In the spectral expansion process, the spatial resolution of the refined GFM_s obtained by combining the satellite-only GFM_s and EGM2008 model is 5'. Because the RET2012 reference topographic model has the same resolution as the refined GFM_s, the reference model serves as a high pass filter, that can filter out low-frequency features from the SRTM data. As a result, the residual terrain height can imply gravity field signals at shorter-scales than the spatial resolution of the refined GFM_s and further compensate for the omission error of the refined GFM_s. The RTM gravitational potential is not harmonic when the computation point below the reference elevation surface. In order to solve the problem of non-harmonic, a harmonic correction usually be done by downward continuation through a Bouguer plate [33,62]. Thus, the harmonic correction for quasi-geoid (or geoid) can be considered as zero, however, harmonic correction for gravity can be considered as $4\pi G\rho\Delta H$ (ΔH represents the height difference between the topography and reference terrain). The choice of the RTM integration radius is crucial. For RTM quasi-geoid height, an integration radius of ~200 km is suitable [49]. Therefore, an integration radius of ~200 km is used herein to determine the RTM quasi-geoid heights. Figure 9 shows the quasi-geoid contribution of the RTM with a resolution of 7.5" × 7.5", with maximum, minimum, mean and standard deviation values of 0.301 m, -0.280 m, 0.001 m and 0.020 m, respectively. It can be seen from the Figure that larger quasi-geoid signals are strongly correlated with topography. However, it should be noted that the RTM quasi-geoid signals may contain some possible implications due to density anomaly and the uncertainties in the harmonic correction [48].

Table 3 shows the quasi-geoid accuracy statistics of different GFM_s in China. From Table 3, without considering the influence of the RTM on the quasi-geoid height, the quasi-geoid accuracies of the refined GFM_s in mainland China are better than 18.5 cm. Among them, the DIR_R6_EGM2008 model has the best accuracy, at 18.1 cm. Compared with the EGM2008 model, the quasi-geoid accuracy of the DIR_R6_EGM2008 model is improved by 8.8 cm. On the other hand, these results also indicate that the quasi-geoid medium-long wavelength accuracy of EGM2008 model in China is poor. Considering the influence of the RTM quasi-geoid, the mainland China quasi-geoid accuracies determined by the refined GFM_s are better than 17.8 cm, and the DIR_R6_EGM2008_RTM model has the optimal quasi-geoid accuracy with a standard deviation of 17.3 cm. Compared with the EGM2008 model, the quasi-geoid accuracy of the DIR_R6_EGM2008_RTM model is improved by 9.6 cm. Compared with the TIM_R5, TIM_R6, DIR_R5 and DIR_R6 models, the quasi-geoid accuracy of the DIR_R6_EGM2008_RTM model is improved by from 0.400 m, 0.391 m, 0.396 m and 0.391 m to 0.178 m, 0.177 m, 0.176 m and 0.173 m, respectively.

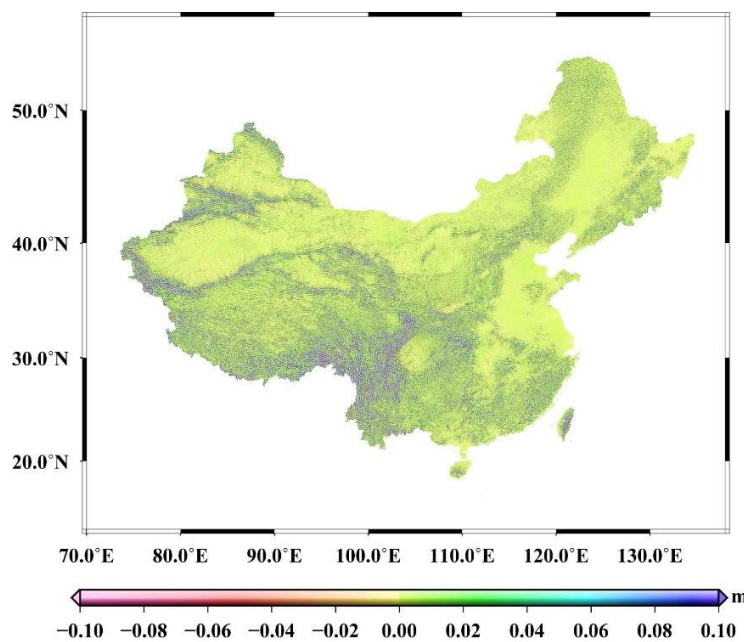


418

Figure 8. Standard deviations of the height anomalies differences between GNSS/levelling and the refined GFMs with varying expansion d/o.

419

420



421

Figure 9. The RTM contribution to quasi-geoid height in China.

422

423

424

425

426

427

428

Table 3. Statistics of the height anomaly differences between GNSS/levelling and the GFMs. Unit: (m).

429

Models	Max	Min	Mean	STD
EGM2008	1.162	-2.079	0.061	0.269
DIR_R6	2.624	-2.475	-0.114	0.391
DIR_R5	2.536	-2.507	-0.112	0.396
TIM_R6	2.578	-2.457	-0.107	0.391
TIM_R5	2.549	-2.432	-0.114	0.400
TIM_R5_EGM2008	1.044	-1.804	0.045	0.185
TIM_R6_EGM2008	1.099	-1.806	0.050	0.184
DIR_R5_EGM2008	1.007	-1.689	0.048	0.183
DIR_R6_EGM2008	1.072	-1.787	0.044	0.181
EGM2008_RTM	1.256	-1.981	0.068	0.261
TIM_R5_EGM2008_RTM	1.042	-1.803	0.053	0.178
TIM_R6_EGM2008_RTM	1.097	-1.806	0.058	0.177
DIR_R5_EGM2008_RTM	1.005	-1.688	0.056	0.176
DIR_R6_EGM2008_RTM	1.069	-1.787	0.052	0.173

To validate our results of the refined GFMs, the EIGEN-6C4 [63], GECO [64], SGG-UGM-1 [65] and SGG-UGM-2 [66] models are used. These four higher-degree GFMs are extended to EGM2008 by adding GOCE data to further improve the medium-long wavelength accuracy.

430
431
432
433

Table 4 summaries the statistics for height anomaly differences between GNSS/levelling and four higher-degree GFMs. These models in Table 4 perform better than EGM2008 model in China, which can assume that the largest impact from the contribution of GOCE solution. The EIGEN-6C4 outperforms GECO, SGG-UGM-1, and SGG-UGM-2 models in China, which is mainly due to the differences in use of GOCE data. Compared Table 3 and Table 4, we can find that the refined GFMs outperform EIGEN-6C4, GECO, SGG-UGM-1, and SGG-UGM-2 in mainland China, the major improvement of these models can be attributed to the GOCE data and topography signals.

434
435
436
437
438
439
440
441

The above analysis shows that the quasi-geoid accuracies of the refined GFMs provide better results. Therefore, to determine high-accuracy quasi-geoid in China, combining the EGM2008 and the satellite-only GFM to obtain the refined models is a feasible strategy. In the combination process, the satellite-only GFM using GOCE, GRACE and LAGEOS laser ranging data should be used, which can better meet the quasi-geoid medium-long wavelength signal. On the other hand, the well-distributed and improved surface gravity data for the quasi-geoid determination of China also play a crucial role and need to be considered further in the future.

442
443
444
445
446
447
448
449**Table 4.** Statistics of the height anomaly differences between GNSS/levelling and four higher-degree GFMs. Unit: (m).

450

Models	Max	Min	Mean	STD
EIGEN-6C4	1.007	-1.696	0.048	0.187
GECO	1.579	-1.703	0.041	0.223
SGG-UGM-1	1.003	-1.671	0.052	0.194
SGG-UGM-2	1.003	-1.704	0.051	0.191

3.4. Determination for the geopotential value of Chinese height datum

451

The geopotential $W_0=62636853.4 \text{ m}^2\text{s}^{-2}$ adopted as reference level for the ITRS is used herein. Based on the GFM, the vertical datum geopotential value for China is determined. Thus, the vertical datum in China is connected into the ITRS.

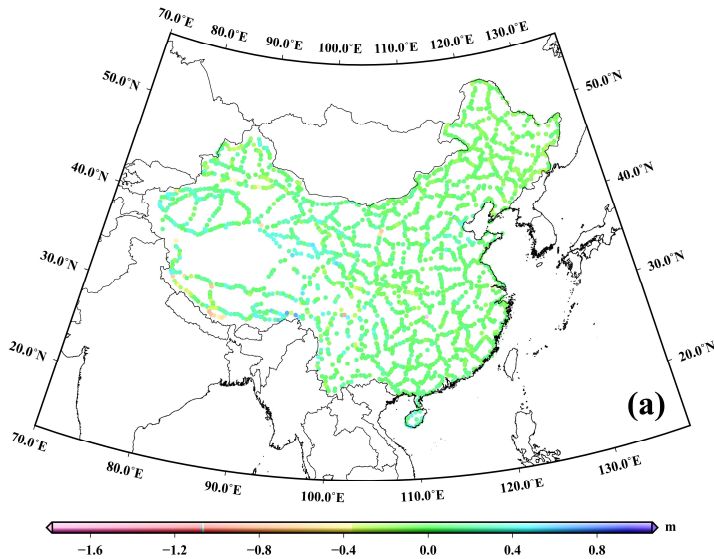
452
453
454

In the analysis presented in section 4.3, we conclude that the DIR_R6_EGM2008_RTM model have optimal quasi-geoid accuracy in China. Therefore,

455
456

we choose this model to derive the Chinese height datum geopotential value. According to Equation (4), we can get vertical offsets values of each GNSS/levelling point. Figure 10(a) represents the height anomaly differences between the GNSS/levelling and the DIR_R6_EGM2008 RTM model in China, thus providing the spatial distribution for the vertical datum offsets. However, it can be found from the Figure10(a) that the discrepancies exist in mainland China. The vertical offsets have certain discrepancies due to the influence of various factors. Among them, systematic error is a major contributor. Therefore, the planar corrections surface is used further through Equations (11). Then, we can derive vertical offsets after applying the correction surfaces by Equation (15). Figure10(b) shows correction surface at GNSS-levelling points. Figure10(c) shows vertical offsets after applying the correction surfaces. It can be seen from Figure10(b) that there are certain east-west systematic errors in China, the maximum error is about 12.2 cm. Systematic errors mainly contain errors in the GFM and levelling, The maximum first-order leveling error in China is only about 3.57 cm after height networks adjustment [32]. Therefore, we can conclude that major systematic effect contributor on the estimation of the height datum geopotential values of China mainly comes from GFM error, the systematic errors from GFM is more obvious in the western China.

The systematic errors influence on the determination of the Chinese height datum geopotential values is evaluated. The results with and without consideration of systematic error effect are compared, as shown in Table 5. Table 5 presents the numerical results of both scenarios based on DIR_R6_EGM2008 RTM model. As shown in the Table 5, we can find that there is a minor improvement of 0.06 m^2s^{-2} for DIR_R6_EGM2008 RTM model when considering the planar corrections. Finally, the geopotential value for the Chinese height datum is derived to be equal to 62636853.29 m^2s^{-2} based on the DIR_R6_EGM2008 RTM model considering planar corrections.



482

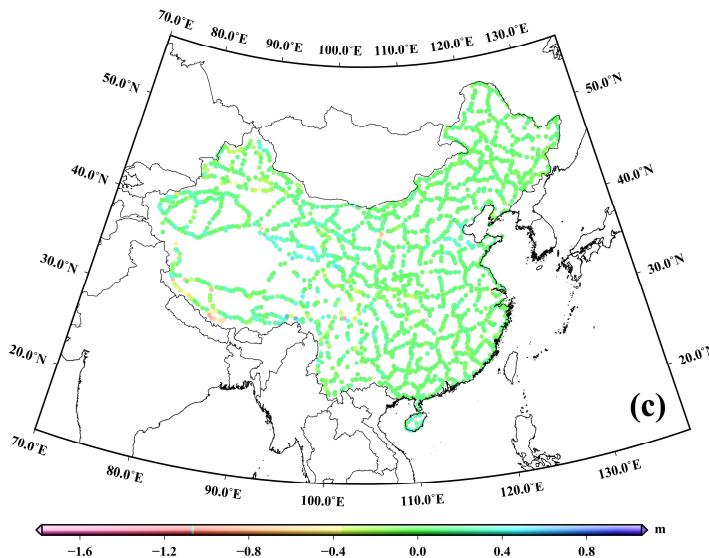
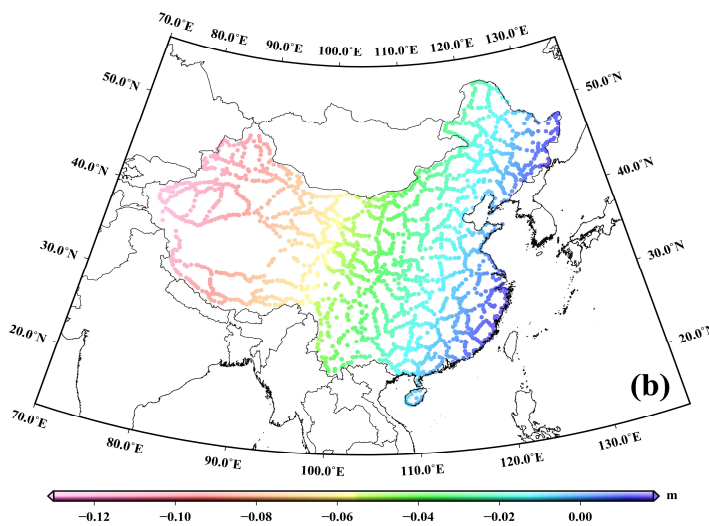


Figure 10. (a) Vertical offsets distribution without applying planar correction surface, (b) Correction surface at GNSS-levelling stations, and (c) vertical offsets distribution after applying the planar correction.

Table 5. Statistics of the without-planar corrections and with-planar corrections scenarios for the height daum geopotential value in China based on DIR_R6_EGM2008 RTM model. Unit: ($m^2 s^{-2}$).

Model	Scenarios	Max	Min	Mean	STD
DIR_R6_EGM2008_RT	without-planar corrections	62636870.86	62636842.93	62636852.89	1.75
	with-planar corrections	62636870.88	62636843.31	62636853.29	1.69

4. Discussion

We use the refined GFMs to preliminarily derive the geopotential value of the Chinese height datum by utilizing the latest normal height results. The refined GGMs provide obvious accuracy improvement advantage and provide guidance for developing a high-accuracy quasi-geoid in China. Prior to this work, He et al. [20] determined the geopotential value of China's height datum as $62636853.47 m^2 s^{-2}$, which fits well with our value of

485

486

487

490

491

492

493

494

495

62636853.29 m²s⁻² considering the standard deviation. The geopotential value of Chinese height datum is determined by utilizing latest national first-order levelling network and GNSS points in this paper, which is representative to some extent.

We can expect that the refined GFM can provide a guidance for determining the quasi-geoid or the geopotential value of the Chinese height datum. However, the combination of the satellite-only GFM with the EGM2008 in this study is by a pure complementation of the spherical harmonic coefficients at a specific degree, which is different from rigorous combination that is done on the basis of the normal equations and co-variance by a least-squares. In the next step, the rigorous combination will be considered to derived the refined GFMs. In addition, the well-distributed surface gravity data for determining the geopotential value of the Chinese height datum also play a crucial role and need to be considered further.

5. Conclusions

In this paper, the theory, method and application for deriving the height datum geopotential value are studied. The refined GFM are proposed to derive the geopotential value of Chinese height datum, aiming to connect Chinese vertical datum to the ITRS. In addition, the effects of the spectral accuracy of GFMs, the omission error of the GFMs and systematic effects on the estimation of the geopotential value of the Chinese height datum are also investigated. The main conclusions are as follows:

The spectral accuracies for satellite-only GFMs and EGM2008 models are estimated. The results show that the satellite-only GFMs have higher medium-long wavelength accuracies than the EGM2008 model, but the maximum expansion degree of these satellite-based models is limited and there are certain omission errors as a result of the gravity field attenuation at the height of satellite orbit. The omission errors of satellite-based GFMs reach the decimeter level in mainland China and cannot be ignored.

To compensate for the omission error in satellite-only GFMs, a spectral expansion approach is proposed to derive the refined GFMs by combining the EGM2008 and the satellite-only GFMs. Because the degree errors of the satellite-only GFMs increase with the increase in degree, the noise starts to dominate signals at high degree and order. Therefore, it is not reasonable to combine the two directly to determine the refined GFMs and it is very important to choose the optimal degree of combination. We find that 230, 240, 220 and 240 are the optimal combination degree for determining the refined GFMs by combining the TIM_R5, TIM_R6, DIR_R5, and DIR_R6 models with the EGM2008 model, respectively. To consider the influence of higher frequency gravity field signals caused by topography, the RTM is utilized to further compensate for the omission errors in the refined GFMs. The mainland China quasi-geoid accuracies determined by the refined GFMs are better than 17.8 cm, and the DIR_R6_EGM2008 RTM model has an optimal quasi-geoid accuracy with of 17.3 cm.

The systematic error effects for determining the geopotential value of the Chinese height datum are considered. The results show that the refined GFMs show minor improvements when considering the planar corrections. The major systematic effect contributor for determining the Chinese height datum geopotential values mainly come from GFM error. Finally, the Chinese height datum geopotential value is derived to be equal to 62636853.29 m²s⁻² based on the DIR_R6_EGM2008 RTM model when considering planar corrections.

Author Contributions: Conceptualization, P.Z. and L.B.; methodology, P.Z. and L.B.; software, P.Z. and Z.L.; validation, P.Z.; formal analysis, P.Z. and L.B.; investigation, All; resources, Z.L.; writing—original draft preparation, P.Z.; writing—review and editing, L.B., Z.L and L.W.; visualization, P.Z.; supervision, L.W., L.B. and Z.L.; funding acquisition, L.B. and Z.L. All authors have read and agreed to the published version of the manuscript.	547 548 549 550 551
Funding: The research was funded by the National Natural Science Foundation of China (Grant Nos. 42174102, 42192535, and 41931076), the National Key Research and Development Program of China (Grant No. 2016YFB0501405), and the Basic Frontier Science Research Program of Chinese Academy of Sciences (Grant No. ZDBS-LY-DQC028).	552 553 554 555
Data Availability Statement: The global Earth Models can be downloaded from ICGEMs (http://icgem.gfz-potsdam.de/tom_longtime/ , accessed on 30 April 2021) and SRTM data can be derived from NASA (https://srtm.csi.cgiar.org/ , accessed on 20 April 2021). In addition, the GNSS/levelling data can be obtained request up on the author.	556 557 558 559
Acknowledgments: We would thank International Centre for Global Earth Models and NASA Shuttle Radar Topographic Mission for providing us with the GFMs and the digital terrain model data, respectively.	560 561 562
Conflicts of Interest: The authors declare no conflict of interest.	563
References	564
1. Barzaghi, R.; De Gaetani, C.I.; Betti, B. The worldwide physical height datum project. <i>Rend. Fis. Acc. Lincei.</i> 2020 , <i>31</i> , 27–34.	565
2. Sánchez, L.; et al. Advances in the realisation of the International Height Reference System. In Proceedings of IUGG. Gen. Assem., Brazil, Nov. 12–14, Nov., 2019.	566 567
3. Sánchez, L., Barzaghi, R. Activities and plans of the GGOS Focus Area Unified Height System. In Proceedings of IUGG. Gen. Assem., Canada, 14. Jul., 2019.	568 569
4. Drewes, H. Reference Systems, Reference Frames, and the Geodetic Datum-Basic Considerations. In Observing our Changing Earth; Sideris, M.G., ed.; Springer: Perugia, Italy, 2009; Volume 133, pp. 3–9.	570 571
5. Drewes, H.; Kuglitsch, F.I.; Adám, J.; Rózsa, S. The Geodesist’s Handbook 2016. <i>J. Geod.</i> 2016 , <i>90</i> , 907–1205.	572
6. Ihde, J.; Sánchez, L.; Barzaghi, R.; et al. Definition and proposed realization of the international height reference system (IHRS). <i>Surv. Geophys.</i> 2017 , <i>38</i> (3), 549–570.	573 574
7. Sánchez, L.; Ågren, J.; Huang, J.; Wang, Y.M.; et al. Strategy for the realisation of the International Height Reference System (IHRS). <i>J. Geod.</i> 2021 , <i>95</i> , 33.	575 576
8. Gerlach, C.; Rummel, R. Global height system unification with GOCE: a simulation study on the indirect bias term in the GBVP approach. <i>J. Geod.</i> 2013 , <i>87</i> (1), 57–67.	577 578
9. Amjadiparvar, B.; Rangelova, E.; Sideris, M.G. The GBVP approach for vertical datum unification: recent results in North America. <i>J. Geod.</i> 2016 , <i>90</i> (1), 45–63.	579 580
10. Ophaug, V.; Gerlach, C. On the equivalence of spherical splines with least-squares collocation and stokes's formula for regional geoid computation. <i>J. Geod.</i> 2017 , <i>91</i> (11), 1–16.	581 582
11. Sánchez, L.; Sideris, M.G. Vertical datum unification for the International Height Reference System (IHRS). <i>Geophys. J. Int.</i> 2017 , <i>209</i> (2), 570–586.	583 584
12. Ebadi, A.; Ardalani, A.; Karimi, R. The Iranian height datum offset from the GBVP solution and spirit-leveling/gravimetry data. <i>J. Geod.</i> 2019 , <i>93</i> (8), 1207–1225.	585 586
13. Zhang, P.; Bao, L.; Guo, D.; et al. Estimation of Vertical Datum Parameters Using the GBVP Approach Based on the Combined Global Geopotential Models. <i>Remote. Sens.</i> 2020 , <i>12</i> (24), 4137.	587 588
14. Hayden, T.; Amjadiparvar, B.; Rangelova, E.; Sideris, M.G. Estimating Canadian vertical datum offsets using GNSS/levelling benchmark information and GOCE global geopotential models. <i>J. Geod. Sci.</i> 2012 , <i>2</i> (4), 257–269.	589 590
15. Gruber, T.; Gerlach, C.; Haagmans, R. Intercontinental height datum connection with GOCE and GPS-levelling data. <i>J. Geod. Sci.</i> 2012 , <i>2</i> (4), 270–280.	591 592
16. Gomez, M.E.; Pereira, R.A.D.; Ferreira, V.G.; et al. Analysis of the Discrepancies Between the Vertical Reference Frames of Argentina and Brazil. In IAG 150 Years; Rizos, C., Willis, P., Eds.; Springer International Publishing: Cham, Switzerland, 2015 ; Volume 143, 289–295.	593 594 595
17. Grombein, T.; Seitz, K.; Heck, B. On High-Frequency Topography-Implied Gravity Signals For a Height System Unification Using GOCE-based Global Geopotential Models. <i>Surv. Geophys.</i> 2016 , <i>38</i> (2), 1–35.	596 597
18. Li, J.; Chu, Y.; Xu, X. Determination of Vertical Datum Offset between the Regional and the global Height Datum. <i>Acta Geodaetica et Cartographica Sinica</i> 2017 , <i>46</i> (10), 1262–1273.	598 599
19. Vergos, G.S.; Erol, B.; Natsiopoulos, D.A.; Grigoriadis, V.N.; Tziavos, I.N. Preliminary results of GOCE-based height system unification between Greece and turkey over marine and land areas. <i>Acta Geod. Geophys.</i> 2018 , <i>53</i> (2), 61–79.	600 601

20. He, L.; Chu, Y.; Xu, X.; Zhang, T. Evaluation of the GRACE/GOCE Global Geopotential Model on estimation of the geopotential value for the China vertical datum of 1985. *Chinese J. Geophys.* **2019**, *62*(6), 2016–2026. 602
603
21. Kelly, C.I.; Andam-Akorful, S.A.; Hancock, C.; Laari, P.; Ayer, J. Global gravity models and the Ghanaian Vertical Datum: challenges of a proper definition. *Surv. Rev.* **2019**, *53*(376). 604
605
22. Zhang, P.; Bao, L.; Guo, D.; Li, Q. Estimation of the height datum geopotential value of Hong Kong using the combined global geopotential models and GNSS/levelling data. *Surv. Rev.* **2021**, *(2)*, 1–11. 606
607
23. Tapley, B.D.; Bettadpur, S.; Watkins, M.; Reigber, C. The gravity recovery and climate experiment: mission overview and early results. *Geophys. Res. Lett.* **2004**, *31*(9), L09607. 608
609
24. Drinkwater, M.R.; Floberghagen, R.; Haagmans, R.; Muñiz, D.; Popescu, A. GOCE: ESA’s first earth explorer core mission. In Earth gravity field from space—from sensors to Earth science; Beutler, G. ed.; Kluwer Academic Publishers: Bern, Switzerland, **2003**; Volume 108, pp. 419–432. 610
611
612
25. Hirt, C.; Gruber, T.; Featherstone, W.E. Evaluation of the first GOCE static gravity field models using terrestrial gravity, vertical deflections and EGM2008 quasigeoid heights. *J. Geod.* **2011**, *85*, 723–740. 613
614
26. Tziavos, I.N.; Vergos, G.S.; Grigoriadis, V.N.; Tzanou, E.A.; Natsiopoulos, D.A. Validation of GOCE/GRACE Satellite Only and Combined Global Geopotential Models Over Greece in the Frame of the GOCESeaComb Project. In IAG 150 Years; Rizos, C., Willis, P., Eds.; Springer International Publishing: Cham, Switzerland, **2015**; Volume 143, 297–304. 615
616
617
27. Gruber, T.; Visser, P.N.A.M.; Ackermann, C.; Hosse, M. Validation of GOCE gravity field models by means of orbit residuals and geoid comparisons. *J. Geod.* **2011**, *85*(11), 845–860. 618
619
28. Kaula, W.M. Theory of satellite geodesy; Blaisdell: Toronto, USA, 1966. 620
29. Forsberg, R. Modelling of the fine-structure of the geoid: methods, data requirements and some results. *Surv. Geophys.* **1993**, *14*, 403–418. 621
622
30. Denker, H. Regional Gravity Field Modeling: Theory and Practical Results. In Sciences of Geodesy – II. Innovations and Future Developments; Xu, G., ed.; Springer: Heidelberg, Germany, 2013; pp. 185–182. 623
624
31. Tscherning, C.C.; Rapp, R.H. Closed covariance expressions for gravity anomalies, geoid undulations, and deflections of the vertical implied by anomaly degree variance models. Reports of the Department of Geodetic Science, the Ohio State University, 1974. 625
626
627
32. Wang, W.; Guo, C.; Li, D.; Zhao, H. Elevation change analysis of the national first order leveling points in recent 20 years. *Acta Geodaetica et Cartographica Sinica* **2019**, *48*(1), 1–8. 628
629
33. Forsberg, R. A Study of Terrain Reductions, Density Anomalies and Geophysical Inversion Methods in Gravity Field Modelling. Scientific report No.5, the Ohio State University, 1984. 630
631
34. Hirt, C.; Featherstone, W.E.; Marti, U. Combining EGM2008 and SRTM/DTM2006.0 residual terrain model data to improve quasigeoid computations in mountainous areas devoid of Gravity Data. *J. Geod.* **2010**, *84*(9), 557–567. 632
633
35. Hirt, C.; Kuhn, M.; Featherstone, W.E.; Göttl, F. Topographic/isostatic evaluation of new-generation GOCE gravity field models. *J. Geophys. Res.* **2012**, *117*, B05407. 634
635
36. Hirt, C.; Bucha, B.; Yang, M.; Kuhn, M. A numerical study of residual terrain modelling (RTM) techniques and the harmonic correction using ultra-high degree spectral gravity modelling. *J. Geod.* **2019**, *(7)*, 1–18. 636
637
37. Yang, M.; Hirt, C.; Rexer, M.; Pail, P.; Yamazaki, D. The tree canopy effect in gravity forward modelling. *Geophys. J. Int.* **2019**, *219*, 271–289. 638
639
38. Altamimi, Z.; Rebischung, P.; Métivier, L.; Collilieux, X. ITRF2014: a new release of the International Terrestrial Reference Frame modeling nonlinear station motions. *J. Geophys. Res. Solid Earth* **2016**, *121*, 6109–6131. 640
641
39. Ekman, M. Impacts of geodynamic phenomena on systems for height and gravity. *Bull. Géod.* **1989**, *63*(3), 281–296. 642
40. Gruber, T.; Abrikosov, O.; Hugentobler, U. GOCE standards. Prepared by the European GOCE Gravity Consortium EGG-C. **2014**. Available online: https://earth.esa.int/documents/10174/1650485/GOCE_Standards (accessed on 1 June 2021). 643
644
41. Pavlis, N.K.; Holmes, S.A.; Kenyon, S.C.; et al. The development and evaluation of the earth gravitational model 2008(EGM2008). *J. Geophys. Res.* **2012**, *118*(5). 645
646
42. Brockmann, J.M.; et al. EGM_TIM_RL05: An independent geoid with centimeter accuracy purely based on the GOCE mission. *Geophys. Res. Lett.* **2014**, *41*(22), 8089–8099. 647
648
43. Brockmann, J.M.; Schubert, T.; Schuh, W.D. An Improved Model of the Earth’s Static Gravity Field Solely Derived from Reprocessed GOCE Data. *Surv. Geophys.* **2021**, *42*, 277–316. 649
650
44. Bruinsma, S.L.; et al. ESA’s satellite-only gravity field model via the direct approach based on all GOCE data. *Geophys. Res. Lett.* **2014**, *41*(21), 7508–7514. 651
652
45. Förste, C.; Abrikosov, O.; Bruinsma, S., et al. ESA’s Release 6 GOCE gravity field model by means of the direct approach based on improved filtering of the reprocessed gradients of the entire mission (GO_CONS_GCF_2_DIR_R6). Available online: <https://doi.org/10.5880/ICGEM.2019.004> (accessed on 14 May 2021). 653
654
655
46. Jarvis, A.; Reuter, H.I.; Nelson, A.; et al. Hole-filled SRTM for the globe Version 4, Available from the CGIAR-SXI SRTM 90m database. **2008**. Available online: <http://srtm.csi.cgiar.org> (accessed on 14 April 2021). 656
657
47. Tozer, B.; Sandwell, D.T.; Smith, W. Global Bathymetry and Topography at 15 Arc Sec: SRTM15+, *Earth Space Sci.* **2019**, *6*, 1847–1864. 658
659

48. Hirt, C.; Claessens, S.; Fecher, T.; Kuhn, M.; Pail, R.; Rexer, M. New ultrahigh-resolution picture of earth's gravity field. *Geophys. Res. Lett.*, **40**(16), 4279–4283. 660
661
49. Hirt, C. RTM gravity forward-modeling using topography/bathymetry data to improve high-degree global geopotential models in the coastal zone. *Mar. Geod.* **36**(2), 1–20. 662
663
50. Hirt, C.; Kuhn, M.; Featherstone, W.E.; Göttl, F. Topographic/isostatic evaluation of new-generation GOCE gravity field models. *J. Geophys. Res.* **117**, B05407. 664
665
51. Moritz, H. Geodetic reference system 1980. *J. Geod.* **2000**, *74*:128–133. 666
52. Sánchez, L.; et al. A conventional value for the geoid reference potential W_0 . *J. Geod.* **2016**, *90*(9), 815–835. 667
53. Yang, M.; Hirt, C.; Tenzer, R.; Pail, R. Experiences with the use of mass-density maps in residual gravity forward modelling. *Stud. Geophys. Geod.* **2018**, *62*. 668
669
54. Nagy, D.; Papp, G.; Benedek, J. The gravitational potential and its derivatives for the prism. *J. Geod.* **2000**, *74*(7–8), 552–560. 670
55. Kotsakis, C.; Katsambalos, K.; Ampatzidis, D. Estimation of the zero-height geopotential level W_0 in a local vertical datum from inversion of co-located GPS, leveling and geoid heights: a case study in the Hellenic islands. *J. Geod.* **2012**, *86*, 423–439. 671
672
56. Gruber, T.; Willberg, M. Signal and error assessment of GOCE based high resolution gravity field models. *J. Geod. Sci.* **2019**, *9*(1), 71–86. 673
674
57. Vu, D.T.; Bruinsma, S.; Bonvalot, S.; Remy, D.; Vergos, G.S.A Quasigeoid-Derived Transformation Model Accounting for Land Subsidence in the Mekong Delta towards Height System Unification in Vietnam. *Remote Sens.* **2020**, *12*, 817. 675
676
58. Voigt, C.; Denker, H. Validation of GOCE gravity field models in Germany. In Assessment of GOCE geopotential models; Huang, J.; Reguzzoni, M.; Gruber, T.; eds.; Newton's Bulletin: Heidelberg, Germany, **2015**; pp. 37–48. 677
678
59. Hofmann-Wellenhof, B.; Moritz, H. Physical Geodesy; Springer: Wien, USA, **2006**. 679
60. Ustun, A.; Abbak, R. On global and regional spectral evaluation of global geopotential models. *J. Geophys. Eng.* **2010** *7*(4), 369. 680
61. Gruber, T.; Willberg, M. Signal and error assessment of GOCE based high resolution gravity field models. *J. Geod. Sci.* **2019**, *9*(1), 71–86. 681
682
62. Forsberg, R.; Tscherning, C.C. Topographic effects in gravity field modelling for BVP. In Geodetic Boundary Value Problems in View of the One Centimeter Geoid; Sansó, F.; Rummel, R., Eds.; Springer: Heidelberg, Germany, **1997**; pp. 241–272. 683
684
63. Förste, C. et al. EIGEN-6C4 The latest combined global gravity field model including GOCE data up to degree and order 2190 of GFZ Potsdam and GRGS Toulouse. Available online: <https://doi.org/10.5880/icgem.2015.1> (accessed on 14 May 2021). 685
686
64. Gilardoni, M.; Reguzzoni, M.; Sampietro, D. GECO: a global gravity model by locally combining GOCE data and EGM2008. *Stud. Geophys. Geod.* **2016**, *60*, 228–247. 687
688
65. Liang, W.; Xu, X.; Li, J.; Zhu, G. The determination of an ultrahigh gravity field model SGG-UGM-1 by combining EGM2008 gravity anomaly and GOCE observation data. *Acta Geodaetica et Cartographica Sinica* **2018**, *47*(4), 425–434. 689
690
66. Liang, W.; Li, J.; Xu, X.; Zhang, S.; Zhao, Y. A High-Resolution Earth's Gravity Field Model SGG-UGM-2 from GOCE, GRACE, Satellite Altimetry, and EGM2008. *Engineering* **2020**, *6*(8), 860–878. 691
692